ISTITUTO NAZIONALE DI FISICA NUCLEARE - ISTITUTO NAZIONALE DI FISICA NUCLEARE - ISTITUTO NAZIONALE DI FISICA NUCLEARE - ISTITUTO NAZIONALE DI FISICA NUCLEARE - ISTITUTO NAZIONALE DI FISICA NUCLEARE - ISTITUTO NAZIONALE DI

Laboratori Nazionali di Frascati

Sublitted to Nucl. Instr. & Meth.

LNF-90/022(P)
5 aprile 1990

V. Muccifora, N. Bianchi, E. De Sanctis, M. Anghinolfi, P. Corvisiero, P. Levi Sandri, V. Lucherini, E. Polli, A.R. Reolon, G. Ricco, P. Rossi, M. Taiuti, G.M. Urciuoli, A. Zucchiatti:

INTERNAL TARGET EFFECTS IN THE ADONE STORAGE RING

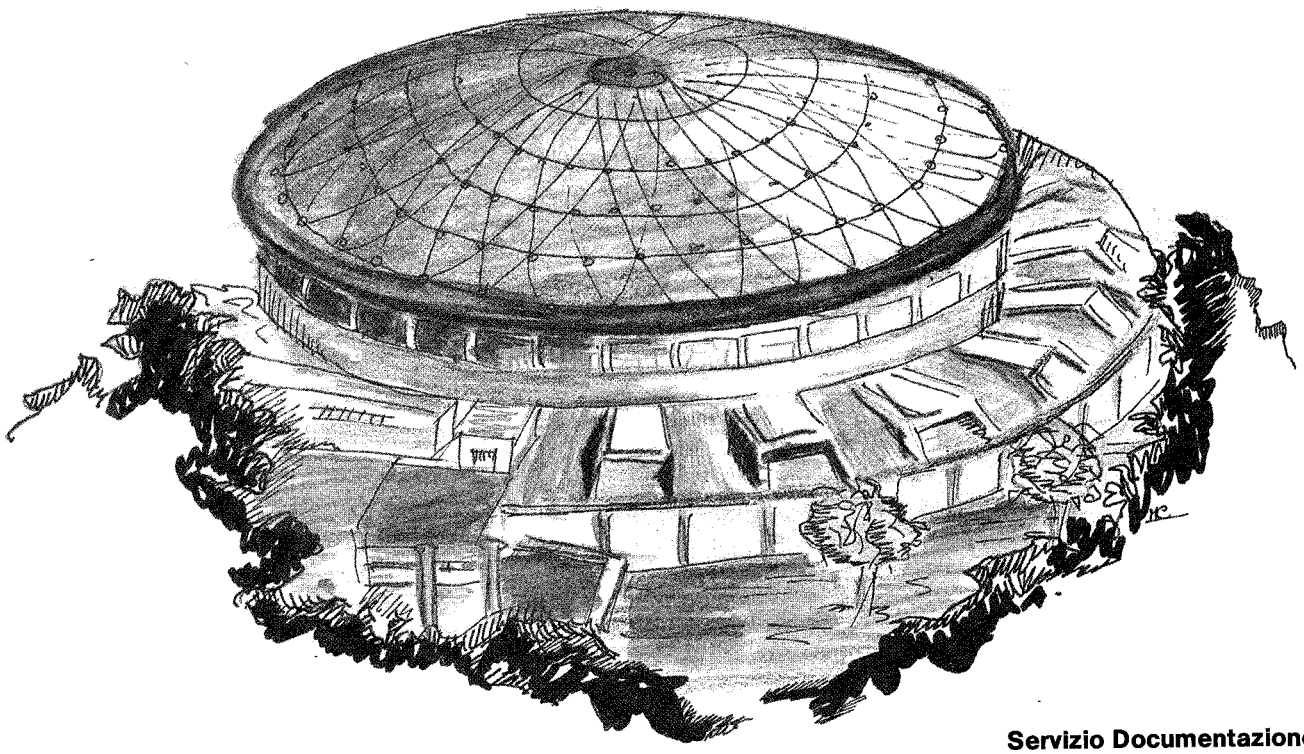

Servizio Documentazione
dei Laboratori Nazionali di Frascati
P.O. Box, 13 - 00044 Frascati (Italy)

INFN - Laboratori Nazionali di Frascati
Servizio Documentazione

LNF-90/022(P)
5 aprile 1990

INTERNAL TARGET EFFECTS IN THE ADONE STORAGE RING

V. Muccifora,[1] N. Bianchi,[1] E. De Sanctis,[1] M. Anghinolfi,[2] P. Corvisiero,[2] P. Levi Sandri,[1] V. Lucherini,[1] E. Polli,[1] A.R. Reolon,[1] G. Ricco,[2] P. Rossi,[1*] M. Taiuti,[2] G.M. Urciuoli,[3] A. Zucchiatti.[2]

[1] INFN-Laboratori Nazionali di Frascati, C.P. 13, I-00044 Frascati
[2] Dipartimento di Fisica dell'Università e INFN-Sezione di Genova, Via Dodecaneso 33, I-16146 Genova
[3] INFN-Sezione Sanità, Viale Regina Margherita 229, I-00185 Roma

ABSTRACT

The effect of a thin (10^{-10}-10^{-8} g·cm^{-2}) Argon jet-target on the beam quality in the ADONE storage ring was studied. The beam emittance growth and electron loss, due to Coulomb scattering, were discussed in the light of the damping mechanism: no effect was expected and observed for electron energies ≥ 500 MeV. The beam lifetime was calculated and measured for different target thickness, and shown to be essentially due to bremsstrahlung processes on the jet-target.

1. INTRODUCTION

The presence of very high currents (100-200 mA) circulating into electron storage rings has suggested that under certain conditions these high beam currents could be used in conjunction with internal targets to achieve reasonable high luminosity under conditions of low background, good energy resolution, negligible multiple scattering with minimal demands for beam from the primary accelerator.[1-3] In its simplest realization the internal target configuration consists of a thin gaseous target located to intercept the beam at a point in the lattice of the storage ring where the circulating particles are highly focused. The high luminosity

---

*Present address: INFN-Sezione Sanità, Viale Regina Margherita 229, I-00185 Roma

is achieved by recirculating the same particles through the target many times per second. The stored energy in the circulating beam is small compared to that dissipated in burying an external beam of comparable luminosity. Consequently, backgrounds and shielding requirements for an internal target facility are modest compared to those for a conventional external beam installation. Therefore, this approach represents an attractive option for performing in a cheap way some of the experiments foreseen in the coming continuous beam accelerators. Cases of particular interest might be in experiments involving polarized targets or the detection of low energy highly ionizing particles such as recoiling target nuclei, deuteron and alfa particles, where energy loss in the target is of prime importance.

A disadvantage of internal targets is that they *heat* the circulating beam, resulting in degraded emittance and reduced beam lifetime for reasonable target thicknesses.Therefore, the target must be thin enough to prevent loss of superior beam quality. The optimal thickness for this kind of applications lies in the range of (1÷10) $ng \cdot cm^{-2}$: a much thicker target would perturb the beam to an uncontrolled level, while a thinner one would lead to an unacceptable low luminosity. In recent years there have been extensive activity in the development of gas targets of useful densities for this aim. A target with the required density range and appropriate geometry is resulted to be a type of condensed gas which consist of large agglomerates of molecules which move at supersonic speed over long distances in high vacuum, without absorption or diffusion by the residual gas.[4-5]

Recently, a molecular Argon cluster-beam has been installed at Frascati on the electron storage ring ADONE with the aim of studying the interaction of circulating electrons with the Argon jet, and producing a monochromatic high energy photon beam through the tagging technique.[6] In this work we analize the effects of the interaction of the Argon jet-target with the ADONE electron beam. In Section 2 we briefly summarize the characteristics of the facility, in Section 3 we discuss the beam loss mechanisms and in Section 4 give the results of measurements of the residual gas levels, beam lifetime, and emittance growth.

2. THE EXPERIMENTAL FACILITY

Fig. 1(a) shows a schematic layout of the positron-electron storage ring, ADONE: the ring is divided into 12 identical regions each consisting of a lattice element (a n=1/2 bending magnet with a quadrupole doublet on each side, which provide focusing in both planes) and a 2.6 m long straight insertions for experiments. The orbit lenght is approximately 105 m, so that a bunch of ultrarelativistic electrons takes about T_0=350 ns to make a round. Electrons are injected into the storage ring at an energy of ≈340 MeV (a few-turn injection will result in about 70 mA current circulating in the ring) and then accelerated to the desired energy by a 51.4 MHz radio-frequency (RF) cavity and kept in orbit by rising the magnetic field of the guiding magnets (this operation requires about 20 s). The RF-cavity groups the circulating electrons into 18 bunches, each ≈1 ns wide and ≈20 ns apart. The maximum energy is 1.5 GeV with energy spread about $6 \cdot 10^{-4}$. In Table I are listed some of the interesting ADONE operating parameters (for more details see Ref. 7).

TABLE I - Parameters of ADONE: the lattice consists of 12 units, with OFDBDFO structure. Each dipole deflects the beam by 30°.

Nominal maximum Energy		1.5 GeV
Maximum current per e^- beam		100 mA
Average vacuum in the ring		10^{-9} Torr
Betatron number		$Q_x=Q_y=3.1$
Length of each straight section		2.6 m
Circumference		105 m
Revolution time		350 ns
Ring radius		16.2 m
Bending radius		5 m
R.F. cavity frequency		51.4 MHz
Harmonic number		18
Damping time	at E_0=1500 MeV	13 ms
	at E_0= 500 MeV	350 ms
Dispersion		ψ=2.05
Natural emittance (at the center of the straight section)	at E_0=1500 MeV	0.24 mm·mrad
	at E_0= 500 MeV	0.027 mm·mrad
Twiss's functions (at the center of the straight section)		$\alpha_x=\alpha_y=0$ $\gamma_x=0.11$ m^{-1}; $\gamma_y=0.305$ m^{-1} M=0.364
Betatron functions		β_x=9m; β_y=3.28m

The target used as a radiator is a condensed beam of molecular Argon[8] which provides a flow of gas at supersonic speed due to the expansion of gas from a vessel at high pressure into the vacuum through a trumpet shaped nozzle of throat diameter 70 μm and semiaperture 3.5°. Argon atoms condensate into microclusters of 10^5-10^6 atoms which minimize the transverse momentum of the atoms and thus the opening angle of the jet. Skimmers further suppress the tail of the density profiles relative to the core. The operating conditions are: inlet pressure and temperature 1÷20 bar and about 300 °K, respectively. From a total flux of ≈10^{20} Ar-atoms·s^{-1} expanding from the nozzle, the collimator system selects about 10^{17}-10^{18} atoms·s^{-1}, which corresponds to a cylindrical beam (∅=6 mm) with thickness of 10^{13}-10^{14} atoms·cm^{-2} (or 1÷10 ng·cm^{-2}) on the path of the electron beam (that is at a distance of ≈25 cm from the nozzle).

The Argon jet target is installed in the straight section n° 5, between consecutive lattice elements, and acts as a radiator to produce a bremsstrahlung photon beam. This is monocromatized by using the tagging tecnique: the recoil electrons are momentum analyzed by the next machine dipole magnet and detected by two arrays of scintillation counters in coincidence (39 counters in each array), placed between the ring vacuum pipe and the dipole magnet flux return joke [Fig. 1 (b)]. The scintillators define 76 energy channels, and have different sizes to give the same photon energy resolution (≈1% at E_0=1500 MeV) over the whole tagging range k=(0.4-0.8)·E_0 (E_0 being the energy of the machine).[6] The photon energy range between 200 and 1200 MeV can be covered with three settings of the end-point energy (E_0= 500, 1000, and 1500 MeV). A photon intensity of about 6·10^7 photons·s^{-1} in the

whole tagging range (that is about $7.5 \cdot 10^5$ photons$\cdot s^{-1}$ per energy channel) is obtained from an average circulating current of about 60 mA, and a jet thickness of ≈ 5 ng$\cdot cm^{-2}$.

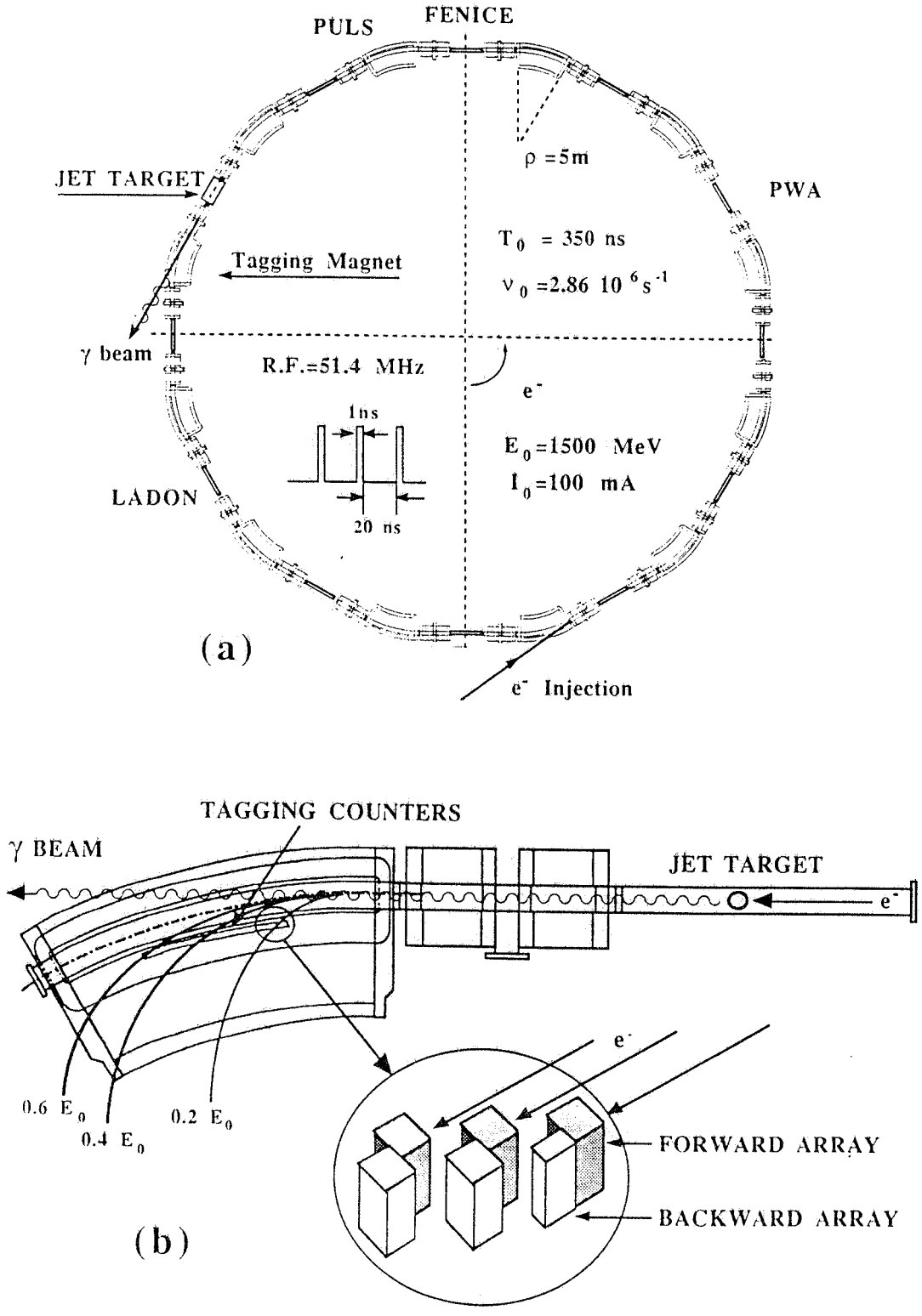

FIG.1 - **(a)** An overview of the ADONE storage ring showing the Argon jet target location. Also shown are the locations of other experimental apparata: the FENICE e^+e^- experiment for measuring the neutron time-like form factor, the LADON laser cavity for the production of a polarized and monochromatic photon beam, and the two sinchrotron ligth stations PULS and PWA. **(b)** An overview of the tagging spectrometer and counters.

3. BEAM LOSS MECHANISMS

After the injection of electrons in the ring and the rise in energy up to the required value, the Argon jet is fired across the ADONE vacuum pipe: this fact cuts down the electron beam lifetime to the value $T_0/(\Sigma\rho x)$, being T_0 the revolution period, Σ the macroscopic removal cross section, and ρ and x the jet density and thickness. Then the cycle is ended by lowering again the field of the magnets to the injection value.

The beam current in the ring decreases as the number of turns (n) around the ring increases. For an initial current I_0, the current after n turns is : $I=I_0 e^{-n\Sigma\rho x}$. The removal cross section, Σ, involves the processes of ionization, bremsstrahlung, elastic electron-electron scattering (Möller scattering) and Coulomb scattering in which electrons lose sufficient energy or are scattered at angles such as to place them outside the phase space of ring.

3.1 Energy losses in the target

For the operating range of jet thicknesses ($1\div10$ ng·cm^{-2}), and electron energies (E_0=500÷1500 MeV), the ionization energy losses in the Argon target are negligible being of the order of 10^{-8} MeV per turn, that is smaller than the average synchrotron energy loss (0.1 MeV per turn) caused by bending in the guiding magnets and, therefore, are provided for by the RF power.

The bremsstrahlung[9] and Möller[10] scattering cross sections for removal of electrons (σ_B and σ_M, respectively) due to the finite energy acceptance bandwidth $\delta=10^{-2}\cdot E_0$ of the RF-cavity, are given by:

$$\sigma_B = \frac{A}{N}\int_{0.01E_0}^{E_0} \frac{1}{X_0}\left(\frac{4}{3}-\frac{4}{3}\frac{k}{E_0}+\left(\frac{k}{E_0}\right)^2\right)\frac{dk}{k} = 8.8\ 10^{-24}\frac{A}{X_0} \quad [cm^2]$$

and:

$$\sigma_M = \int_{0.01E_0}^{E_0} \frac{2\pi Z\, r_0^2}{q^2}\,dq = 2\ 10^{-23}\frac{Z}{E_0} \quad [cm^2]\ ,$$

where X_0 [g·cm^{-2}] and A [g] are the target radiation lenght, and atomic mass, N is the Avogadro number, k the photon energy, r_0 the classical electron radius, q the recoil energy (assumed $<<E_0$, and given in units of mc^2): all the energies are espressed in MeV.

From the previous expressions it follows that the bremsstrahlung cross section is proportional to X_0^{-1} and then to the squared atomic number, Z^2, while the Möller scattering cross section increases linearly with increasing Z and decreasing the energy E_0 of the electron beam. For our Argon jet-target (Z=18) in ADONE, the ratio σ_M/σ_B is about 2% at E_0=500 MeV and lower at higher energies: this makes negligible the effect of Möller scattering on the characteristics of the stored beam. Therefore, the bremsstrahlung in the target is the only process important for energy losses.

For what concerns the bremsstrahlung, electrons radiate low energy photons with high probability, thus loosing a small amount of their energy. When their energy is between the energy resolution of the beam, $\Delta=10^{-3}\cdot E_0$, and the acceptance δ of the ring, they produce an halo whose intensity is about 0.1% of the circulating beam. When their energy is sligtly out of the acceptance of the ring (between δ and 2δ) they are not removed in one turn but spiralize inside the vacuum pipe, and can hit the vacuum chamber somewhere in front of the tagging counters producing an electromagnetic shower. In order to protect the tagging counters from this possible background a beam scraper (a 10 mm thick stainless steel slit) has been installed at a position ≈15 m downstream the gas target. It can be inserted inside the vacuum chamber up to the beam orbit once the injection is completed: measurements performed in different conditions have shown negligible this electromagnetic background.

3.2 Effect of the scattering in the target

Loss for scattering by the Coulomb field of the target atoms occurs when the scattering angle exceeds the acceptance angle of ring. This does not happen for target thickness in the range $10^{-10}\div10^{-8}$ g·cm^{-2}: therefore, in our case, this process may contribute only to the growth of the phase space of electron beam. This effect was evaluated using a Monte Carlo simulation and the single scattering probability distribution given by Craft and Williamson.[11] In this model the scattering process is characterized by two angles: the screening angle χ_α, and the angle χ_c, beyond which the screening can be neglected. For relativistic electrons one has:

$$\chi_\alpha = \chi_\mu\left(1 + 0.04902\chi_\mu\right) \quad \text{[rad], and} \qquad \chi_c^2 = 0.157\, Z\,(Z+1)\,\frac{\rho x}{Ap^2} \quad [\text{rad}^2]$$

where $\chi_\mu = 4.215\cdot10^{-3}\cdot\mu\cdot Z^{1/3}/p$ [rad] is the Born screening angle, μ is a parameter which is adjusted to fit experimental data (in the calculations discussed in this paper the value $\mu=1.8$ was assumed, as suggested by Nigam, Sundareseen and Wu[12], p is the momentum of the incident electron in energy units, Z and A are the target atomic and mass numbers, and ρx is the target thickness.

The relevant parameter for determining the nature of the scattering is Ω, wich represents the mean number of scattering in a single passage through the target. This depends upon the density and atomic number of the target material through the following relation:

$$\Omega = \frac{\chi_c^2}{\chi_\alpha^2} \approx 8837\, Z^{1/3}(Z+1)\frac{\rho x}{\mu^2 A}.$$

For target thickness considered in this report, one is not dealing with multiple scattering but essentially with a single scattering from a screened potential. The probability of scattering, normalized including only the no scattering and one scattering terms, is:[11]

$$F(\vartheta_\alpha,\Omega)=\frac{1}{2\pi(1+\Omega)}\left(\delta_2(\vartheta_\alpha)+\frac{2\Omega}{\left(1+\vartheta_\alpha^2\right)^2}\right),$$

where $\vartheta_\alpha=\vartheta/\chi_\alpha$ is the reduced polar angle, and $\delta_2(\vartheta_\alpha)$ is a two dimensional delta function.

The effect of the internal target on the angular and spatial distributions of the beam was determined by using a computer simulation in wich a large number of particles were tracked through the required number of turns. A first-order transport matrix, T, was used for one revolution around the ring beginning at the target location: then the following equation was used to determine the coordinates (in the radial plane) of an electron when it returned to the target point after a revolution in the ring:

$$\mathbf{x}_{i+1}=T_x(\mathbf{x}_i+\Delta\mathbf{x}_i),$$

where

$$\mathbf{x}_i=\begin{vmatrix} x_i \\ \vartheta_i \end{vmatrix}, \text{ and } \Delta\mathbf{x}_i=\begin{vmatrix} 0 \\ \Delta\vartheta_i \end{vmatrix},$$

are the electron position and angle at the $(i)^{th}$ target crossing, and its change in direction due to scattering.

The computer simulation extracted the position and angle from the intrinsic emittance beam and estimated, at each passage in the target, the possibility of having no scattering or a single scattering. If no scattering occured the electron was transported around the ring for another turn. If the scattering took place, the reduced polar angle ϑ_α was extracted and weighted by the single scattering distribution. Then, by extracting the azimuth angle, we got the projected angle $\Delta\vartheta_i$ of the outgoing electron from the target.

The calculations were made for an Argon jet of 10^{-8} g·cm^{-2} thickness and electron beam energies E_0=1500 MeV and E_0=500 MeV. For E_0= 1500 MeV (500 MeV), 4000 (2000) electrons were tracked over 37000 (10^6) revolutions, corresponding to one damping time of ADONE 13 ms (350 ms). Figs. 2 and 3 show the results obtained: solid lines represent the initial radial distribution and the solid diamonds, with their statistical errors, the final radial distribution. As it is seen, no appreciable emittance growth is observed for the thickness and energies considered.

The calculations were also made for various combinations of the characteristic parameters: specifically six values of Ω (between $5\cdot10^{-4}$ and 10^{-3}) and three values of χ_α ($6.6\cdot10^{-6}$, $1\cdot10^{-5}$, and $2\cdot10^{-5}$ rad). Fig. 4 shows the results obtained: for the range of realistic parameters considered, the following approximate power law dependence on Ω and on χ_α of the emittance growth rate per revolution, $d\varepsilon/dn$ (solid lines in the figure), was observed:

$$\frac{d\varepsilon}{dn}\approx 2.85\,10^{5}\,\Omega^{1.1}\,\chi_\alpha^{2} \quad [\text{mm}\cdot\text{mrad/turn}],$$

which, expressed as a function of time, takes the form:

$$\frac{d\varepsilon}{dt} \approx 8.55\,10^{11}\,\Omega^{1.1}\,\chi_\alpha^{2} \quad [\text{mm·mrad/s}] .$$

Therefore, in the absence of the beam damping the internal target would cause the beam emittance to grow monotonically in time. Taking into account the damping effect, the emittance value ε_{eq} after a damping time τ is:[13]

$$\varepsilon_{eq} = \varepsilon_0 + \frac{d\varepsilon}{dt}\tau ,$$

where ε_0 is the emittance value in the absence of internal target. Since ε_0, $d\varepsilon/dt$, and τ are proportional respectively to E^2, E^{-2}, and E^{-3}, the first term of ε_{eq} increases as E^2, while the second decreases as E^{-5}. These dependences are reflected into the shapes of the curves shown in Fig 5 which give the emittance growth in ADONE without jet target and for four Argon jet thicknesses. As it is seen, in the range of interest for the tagging system (500 MeV<E_0<1500 MeV) the calculations do not foresee any emittance growth up to 10 ng·cm^{-2}.

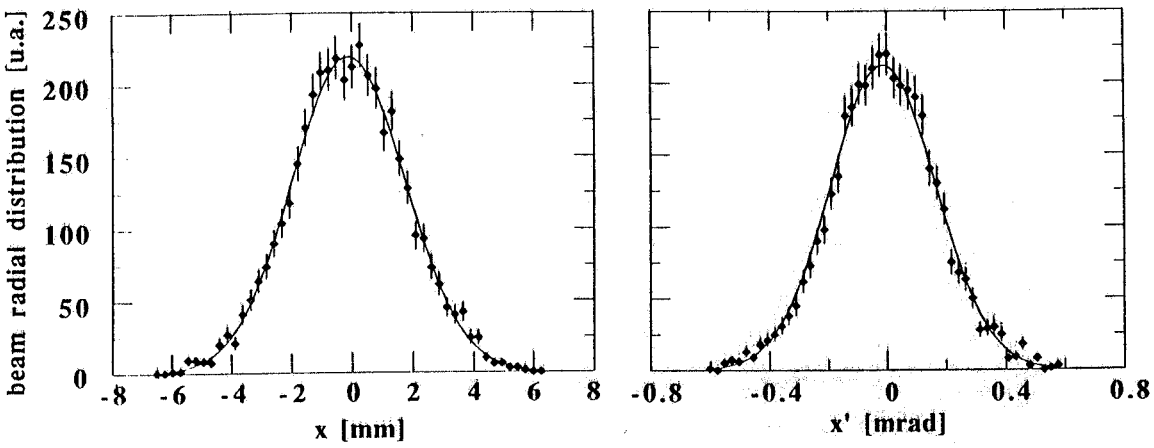

FIG. 2 - Radial beam distributions at 1500 MeV, respectively without the Argon clustered-jet (10 ng·cm^{-2} thickness) [solid lines] and after one damping time of ADONE [solid diamonds], corresponding to 37000 revolutions.

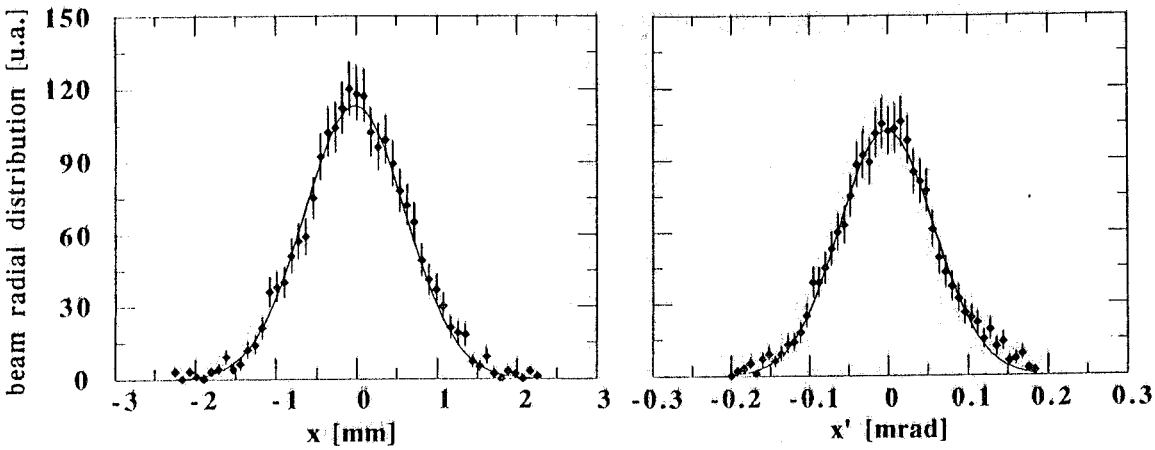

FIG. 3 - Radial beam distributions at 500 MeV, respectively without the Argon clustered-jet (10 ng·cm^{-2} thickness) [solid lines] and after 10^6 revolutions [solid diamonds], corresponding to one damping time of ADONE.

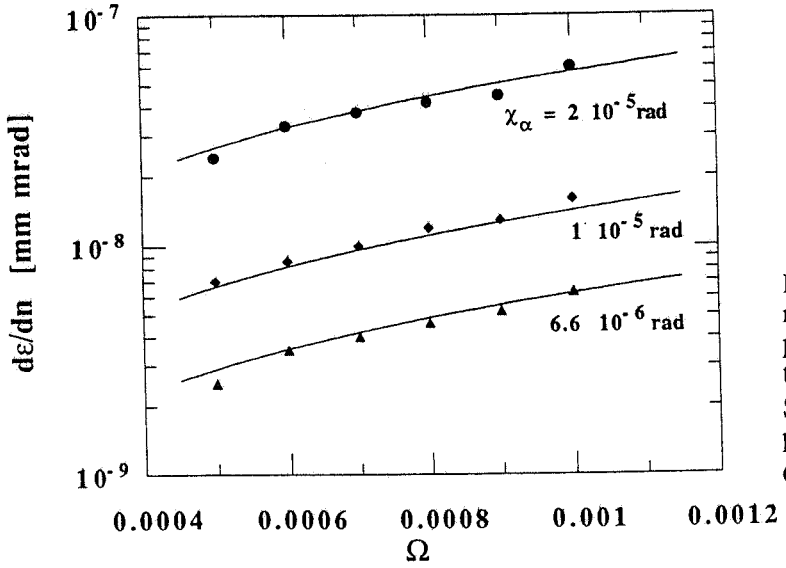

FIG. 4 - Emittance growth rate per revolution versus the scattering probability per revolution (Ω) for three values of the polar angle, χ_α. Solid lines are obtained with the power law dependences on Ω and χ_α described in the text.

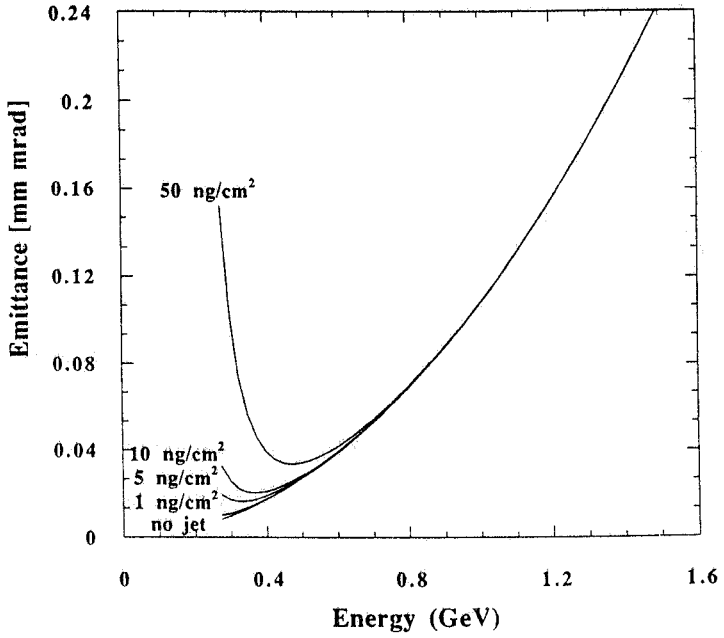

FIG. 5 - ADONE electron beam emittance versus energy for normal conditions (without the Argon clustered-jet) and for four jet thicknesses.

4. EXPERIMENTAL RESULTS

A major concern in the target design arose from the need to limit the pressure increase in the ADONE vacuum pipe to an acceptable level. The vacuum system installed on ADONE to produce the Argon beam is a vertical construction with the differentially pumped source at the top, the interaction chamber at the center and the target-beam dump at the bottom. The system is able to locally confine the gas to a high degree and recover the ring base pressure in a short distance both upstream and downstream from the target. Such increases in the base pressure would add to the effective target thickness and decrease the lifetime of the recirculating beam. In order to contain the pressure rise each time the jet is fired, and to return quickly to normal vacuum levels when the jet is switched off, two 1000 $l \cdot s^{-1}$ turbomolecular pumps were located on the straight section immediately before and after the interaction chamber. The pumping in the rest of the ring is performed by the existing turbo pumps.

Fig. 6 shows the vacuum levels in the straight section where the jet-target is installed for various Argon jet thicknesses measured in different runs: the vacuum in the rest of the ring resulted unaffected. The recovery time to the normal vacuum level $6 \cdot 10^{-10}$ mbar, after the jet was switched off, was about one minute. Furthermore, by comparing the mass spectra from the ADONE residual gas in normal condition and immediately after switching the jet off, we found no changement in the composition of the residual gas.

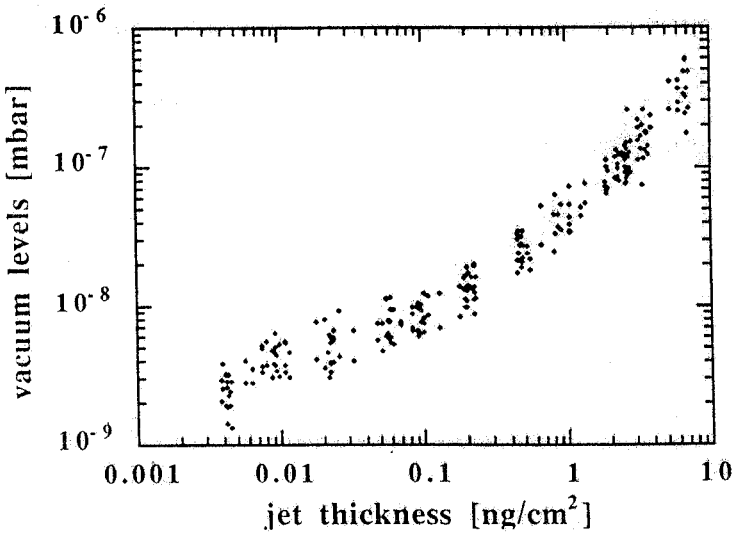

FIG. 6 - Vacuum levels in the straight section where the jet target is installed versus the jet thickness.

As said above, the Argon jet thickness is so small that, at energies higher than 500 MeV, neither the Coulomb scattering nor ionization losses contribute to the beam quality degradation, being the RF-cavity able to compensate for both the growth in divergency and the mean energy losses. Therefore, as for the beam lifetime, the removal cross section involves only those processes of bremsstrahlung in which the electrons loose sufficient energy to place them outside the acceptance band-width δ of the ring. This is easily seen in Fig. 7, where the beam

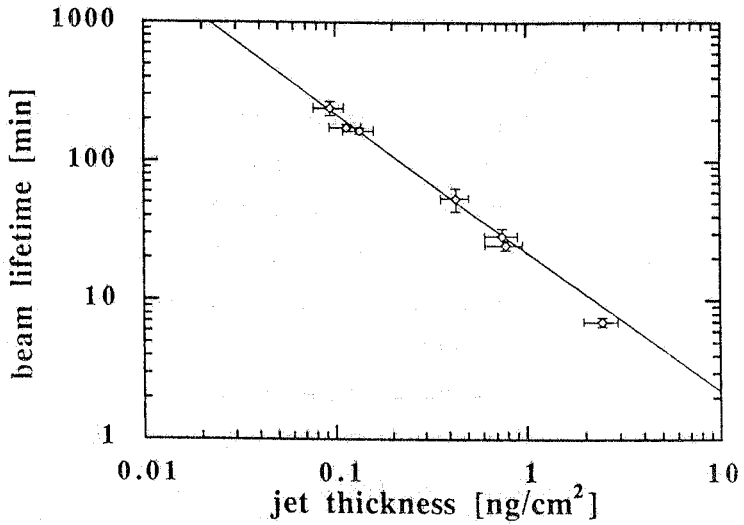

FIG. 7 - ADONE electron beam lifetime, τ, versus the Argon jet thickness, ρx. The solid line is the curve $\tau = T_0/(\Sigma_B \rho x)$: T_0 and Σ_B are respectively the revolution period and the macroscopic bremsstrahlung cross section for removal of electrons.

lifetime values (corrected for the contribution of the residual vacuum) measured for a few jet thicknesses (between 0.1 and 3 $ng \cdot cm^{-2}$) are compared with the result of a calculation performed using the relation $\tau = T_0 / \Sigma_B \cdot \rho x$. The good agreement between experimental points and prediction is a clear validation that the removal cross section, for the range of electron energies and target thickness considered, is the macroscopic bremsstrahlung cross section $\Sigma_B = \sigma_B N/A$.

Finally, we have checked that the effects of the Argon jet on the beam emittance were negligible by observing the beam spot produced by sinchrotron light on a screen for $E_0 = 500$ MeV and jet thickness ≈ 4 $ng \cdot cm^{-2}$: no increase in the cross sectional area of the beam was observed, as foreseen by the calculation.

5. CONCLUSION

We have studied the effects of a thin Argon clustered-jet target on the quality of the electron beam circulating into the ADONE storage ring. It has been shown that, for energies higher than about 500 MeV, both beam loss from Möller, and multiple scattering and emittance growth are negligible and that the limitation on target densities (and thus beam-gas luminosity for internal target physics) is dictated only by loss of electrons by bremsstrahlung processes. Consequently, for a target of atomic number Z and thickness ρx, the beam loss would be proportional to the product $\rho x \cdot Z^2$.

We would like to thank Dr. Miro Preger for enlightnening discussions on the ADONE optics, and Dr. Virgilio Chimenti for continue advise and assistance for vacuum problems.

REFERENCES

1) Proc. Workshop on the Use of Electron Ring for Nuclear Physics, Lund, October 5-7, 1982, Ed.J.O. Adler and B. Schroder.
2) Proc. Workshop on Electronuclear Physics with Internal Targets, SLAC, January 5-8, 1987, Eds. R.G. Arnold and R.C. Minehart SLAC-316,UC-34C (1987).
3) Proc. Topical Conference on Electronuclear Physics with Internal targets, SLAC January 9-12, 1989, Ed. R.G. Arnold, World Scientific.
4) J. Gspann, in Proc. Workshop on the Use of Electron Ring for Nuclear Physics, Lund, October 5-7, 1982, Ed.J.O. Adler and B. Schroder, (1982) p. 85.
5) O.F. Hagena and W. Obert, J. Chem. Phys., 56 (1972) 1793.
6) E. De Sanctis, M. Anghinolfi, N. Bianchi, P. Corvisiero, S. Frullani, G. Garibaldi, G. Gervino, C. Guaraldo, P. Levi Sandri, V. Lucherini, V. Muccifora, E. Polli, A.R. Reolon, G. Ricco, P. Rossi, M. Sanzone, M. Taiuti, G.M. Urciuoli, A. Zucchiatti, Frascati Internal Report, LNF 90/001 (1990).
7) F. Amman et al. in Proc. of 5th International Conference on High Energy Accelerators, Frascati, September 9-16, 1965, Ed. M. Grilli, (1965) p. 703.
8) M. Taiuti M. Anghinolfi, N. Bianchi, P. Corvisiero, E. De Sanctis, E. Durante, S. Frullani, G. Garibaldi, C. Guaraldo, U. Lantero, P. Levi Sandri, V. Lucherini, L. Mattera, V. Muccifora, E. Polli, A.R. Reolon, G. Ricco, P. Rossi, A. Rottura, M. Sanzone, G.M. Urciuoli, U. Valbusa, A. Zucchiatti, Proc. Topical Conference on Electronuclear Physics with Internal targets, SLAC 9-12 January 1989, Ed. R.G. Arnold, World Scientific, p.140.
9) Y.S. Tsai, Rev. Mod. Phys., 46 (1974) 815.
10) W. Heitler, Quantum Theory of Radiation , Clarendon Press (1957)
11) B. Craft and C.F. Williamson, Bates Internal Report, 83-03 (1983).
12) B.P. Nigam, M.K. Sundareseen and Ta-You Wu, Phys. Rev. 115 (1959) 491
13) B. Norum, CEBAF 1985 Summer Study, 12-70 (1985).